

Solar wind temperature anisotropy during Ulysses' first fast latitude scan

Ephrem Tesfaye Desta^{1,2}, R. D. Strauss^{1,3} and N. E. Engelbrecht^{1,3}

¹Center for Space Research, North-West University, Potchefstroom, 2522, South Africa.

²Department of Physics, Addis Ababa University, Addis Ababa, 1176, Ethiopia

³National Institute for Theoretical and Computational Sciences (NITheCS), South Africa.

E-mail: 50156888@mynwu.ac.za

Abstract. Anisotropy is a property of turbulence in solar wind plasma in which velocity and magnetic fields fluctuate along and perpendicular to the ambient magnetic field. In situ measurements confirmed that the solar wind in the inner heliosphere exhibits a temperature anisotropy. The presence of this anisotropy results in magnetohydrodynamic (MHD) waves and instabilities. In this report, we analyze proton temperature anisotropy using Ulysses spacecraft data and investigate the radial variation of the temperature anisotropy for Fire-hose and Mirror instabilities. From Ulysses observations, we find that the Fire-hose instability is dominant in the range between 3 au to 4.5 au.

1 Introduction

The study of solar wind plasma provides crucial insights into the dynamic interactions between the Sun's emission of particles and the interplanetary medium. As the solar wind expands beyond the collision-dominated solar corona, it encounters a largely collisionless plasma that flows supersonically through a weakly inhomogeneous magnetic field region. This magnetic field significantly influences the plasma's behaviour, leading to the development of temperature anisotropies and shaping the overall dynamics of the solar wind [1]. Observations from *Helios* have revealed that at 0.3 astronomical units (au) from the Sun, there are distinct anisotropic and isotropic populations of solar wind plasmas that become indistinguishable at 1 au [2]. This transitional region is known as the polytropic zone, where both isotropic and anisotropic plasmas coexist. The anisotropic cascade in this region is crucial as it facilitates significant energy transfer, especially in magnetized plasmas where large perpendicular wavenumbers (k_{\perp}) are dominant. The particle distribution functions in these plasmas often exhibit anisotropy, particularly in proton temperature, which can drive various instabilities.

Solar wind plasmas are frequently in a turbulent state characterized by a broad spectrum of fluctuations across various wave vectors. This turbulence promotes an ongoing cascade of energy between different wave vectors, leading to an anisotropic cascade in the presence of a background magnetic field (B_0). Theoretical models, simulations and observational data consistently show that energy is preferentially transferred to large values of k_{\perp} , where k_{\perp} is the wave number perpendicular to B_0 . This results in a cascade dominated by perpendicular fluctuations [3, 4].

In low-collisionality plasmas like the solar wind, the particle distribution function can also display anisotropy relative to the magnetic field. For instance, the temperature anisotropy $T_{\perp p}/T_{\parallel p}$, where $T_{\perp p}$ and $T_{\parallel p}$ are the temperatures perpendicular and parallel to the magnetic field, respectively, can drive various plasma instabilities. When $T_{\perp p}/T_{\parallel p} > 1$, the plasma may become unstable to parallel-propagating Alfvén/ion-cyclotron (A/IC) waves or non-propagating mirror modes [5, 6]. Conversely, when $T_{\perp p}/T_{\parallel p} < 1$, the plasma can excite fast-magnetosonic/whistler (FM/W) waves or oblique firehose modes [7, 8]. These instabilities help constrain the temperature anisotropy, driving the plasma toward a marginally stable state [9, 10].

The firehose instability, occurring when $T_{\parallel p} > T_{\perp p}$ is vital in regulating temperature anisotropy in high- β plasmas, where β represents the ratio of plasma pressure to magnetic pressure. This instability has been extensively studied, revealing both parallel and oblique firehose modes as mechanisms that can relax anisotropy and prevent the plasma from becoming excessively elongated along the magnetic field [11, 8]. Observational studies, such as those by [12], have identified thresholds for these instabilities in the solar wind, underscoring their role in shaping proton distribution functions.

Similarly, the mirror instability, triggered when $T_{\perp p} > T_{\parallel p}$, imposes constraints on the perpendicular temperature in the solar wind. This instability is particularly relevant in high- β regions, where it leads to the formation of non-propagating structures that contribute to energy redistribution within the plasma [13, 10]. Additionally, the ion-cyclotron instability, which emerges under similar conditions, has been linked to the generation of Alfvén waves propagating along the magnetic field, further contributing to the turbulent cascade [14].

Understanding the interplay between these instabilities and the turbulent cascade is essential for comprehending the dynamics of the solar wind and other astrophysical plasmas. As the solar wind expands away from the Sun, these processes collectively influence the evolution of temperature anisotropies, resulting in a complex distribution of proton temperatures that reflects the balance between turbulent energy transfer and kinetic instabilities [15].

This paper investigates which instability is dominant while the solar wind plasma expands as function of heliographic latitude and heliocentric distance, by analyzing Ulysses data. This can gain deeper insights into the mechanisms regulating plasma behavior on a kinetic scale, enhancing our understanding of space weather and heliospheric conditions. The paper is organized as follows: section 2 presents dataset, method and results, while section 3 provides the discussion and conclusions.

2 Dataset, Methods and Results

We utilize the proton moments data from the Solar Wind Observations Over the Poles of the Sun [16] electrostatic instrument and we use magnetic field measurements from the magnetic field investigation instrument the Vector Helium, and other Flux Gate Magnetometer [17] experiment. The list of the data is available from NASA's SPDF-Coordinated Data Analysis Web¹ spanning from 1992 January 1 to 1998 December 31 [18]. Figure 1 shows the Ulysses spacecraft trajectory in the plane of radial distance and latitude and solar wind plasma parameters that we analyze in this study. Ulysses explores the region from 1.25 to 5.4 au and encountered mainly fast solar wind, especially at high latitudes, while some slow wind was measured closer to the ecliptic, below 1.5 au and beyond 4.5 au. More dense plasma with slow solar wind was measured around 1.5 au and in the range of 3 au to 4.5 au. This region has a more dense distribution and slow solar wind speed. The slow solar wind is measured in the range beyond 4.5 radial distance and latitude in the range $[60^\circ, -20^\circ]$ as shown in Figure 1.

This timing of the mission has enabled Ulysses to make direct measurements of the high-latitude solar wind coming from the Sun's polar coronal holes, and thus characterise the global structure of the heliosphere during solar minimum conditions when the corona is in its simplest configuration.

The Chew-Goldberger-Low model (CGL) fluid theory gives the two adiabatic equations of states, neglecting the heat flux vector, which are given by [19] as

$$\frac{d}{dt} \left(\frac{P_{\perp}}{nB} \right) = 0, \quad \text{and} \quad \frac{d}{dt} \left(\frac{P_{\parallel} B^2}{n^3} \right) = 0, \quad (1)$$

These would lead to an evolution for the parallel and perpendicular (with respect to \mathbf{B}) particle temperatures, T_{\parallel} and T_{\perp} as:

$$T_{\perp} \propto B \quad \text{and} \quad T_{\parallel} \propto n^2/B^2, \quad (2)$$

where B is the magnitude of the ambient magnetic field and n is the plasma density. In the case of CGL double-adiabatic expansion, with a constant flow velocity and in a radial magnetic field, these parameters would change with the radial distance R as $B \propto n \propto R^{-2}$; consequently, the relations in (2) predict the development of strong temperature anisotropy

$$\frac{T_{\perp}}{T_{\parallel}} \propto R^{-2} \quad \text{and} \quad \beta_{\parallel} \propto R^2, \quad (3)$$

A useful technique for studying solar wind temperature anisotropy is examining how $T_{\perp p}/T_{\parallel p}$ varies as a function of plasma- β

$$\frac{T_{\perp p}}{T_{\parallel p}} = 1 + \frac{a}{(\beta_{\parallel} - c)^b}. \quad (4)$$

¹<https://cdaweb.gsfc.nasa.gov/index.html>

Following [9], for our instability analysis we choose the fitting parameters where (a,b,c) are given by (0.43,0.42,-0.0004) for proton cyclotron instability (PCI), (0.77,0.76,-0.016) for mirror instability (MI), and (-0.47,0.53,0.59) for parallel firehose instability (PFH), and $\beta_{\parallel} = 2\mu_0 n_p k_B T_{\parallel p} / B_0^2$.

The radial profile and plasma properties of the spacecraft that we examine in this work are displayed in Figure 1.

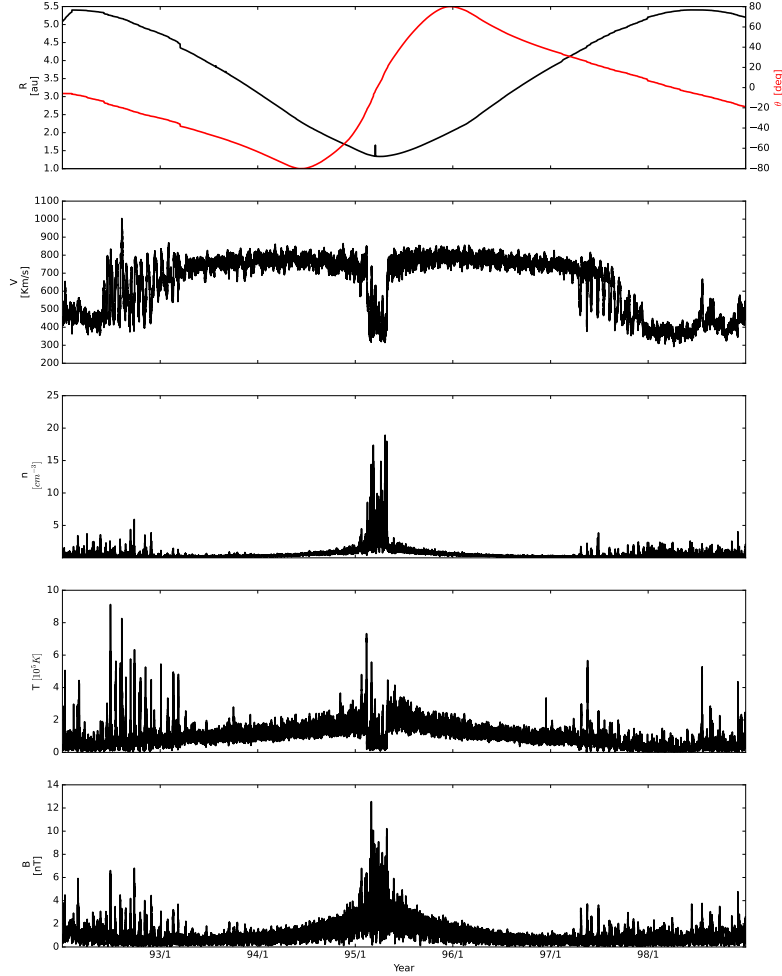


Figure 1: An overview of key parameters measured by Ulysses for this study: (top panel) heliocentric range (black) and heliolatitude (red) trajectory; (second panel) Solar wind speed; (third panel) plasma number density; (Fourth panel) temperature; (bottom panel) magnetic field of Ulysses.

3 Discussion and Conclusion

The Ulysses observations are consistent with the parallel fire hose instability in the range between 3 au and 4.5 au. In this region, our result shows that the temperature anisotropy ratio in the range $0.6 < T_{\perp p} / T_{\parallel p} < 0.9$ is in the mean stream component of the solar wind. In this range, we find that the average of $T_{\perp p} / T_{\parallel p}$ is 0.85, which has similar results to studies by [20, 21]. Figures 2 show the evolution of radial (R) information of temperature anisotropy and the region of instability that approaches the fire-hose instability with increasing distance in the range of 3 au to 5.41 au.

Based on Helios and Ulysses observation in the range of proton temperature anisotropy evolution from 0.3 to 2.5 au [22] indicated that both the slow and fast wind are found to approach the fire hose instability regions with increasing distance. Similarly, based on the report by [23], the fire hose instability plays a major role in constraining the proton anisotropy during solar wind expansion, and with increasing distance, the wind approaches the fire hose instability region. Based on Ulysses' observations and empirical correlations of plasma parameters [23] indicated that a large portion of proton distribution in the solar wind has fire hose instability.

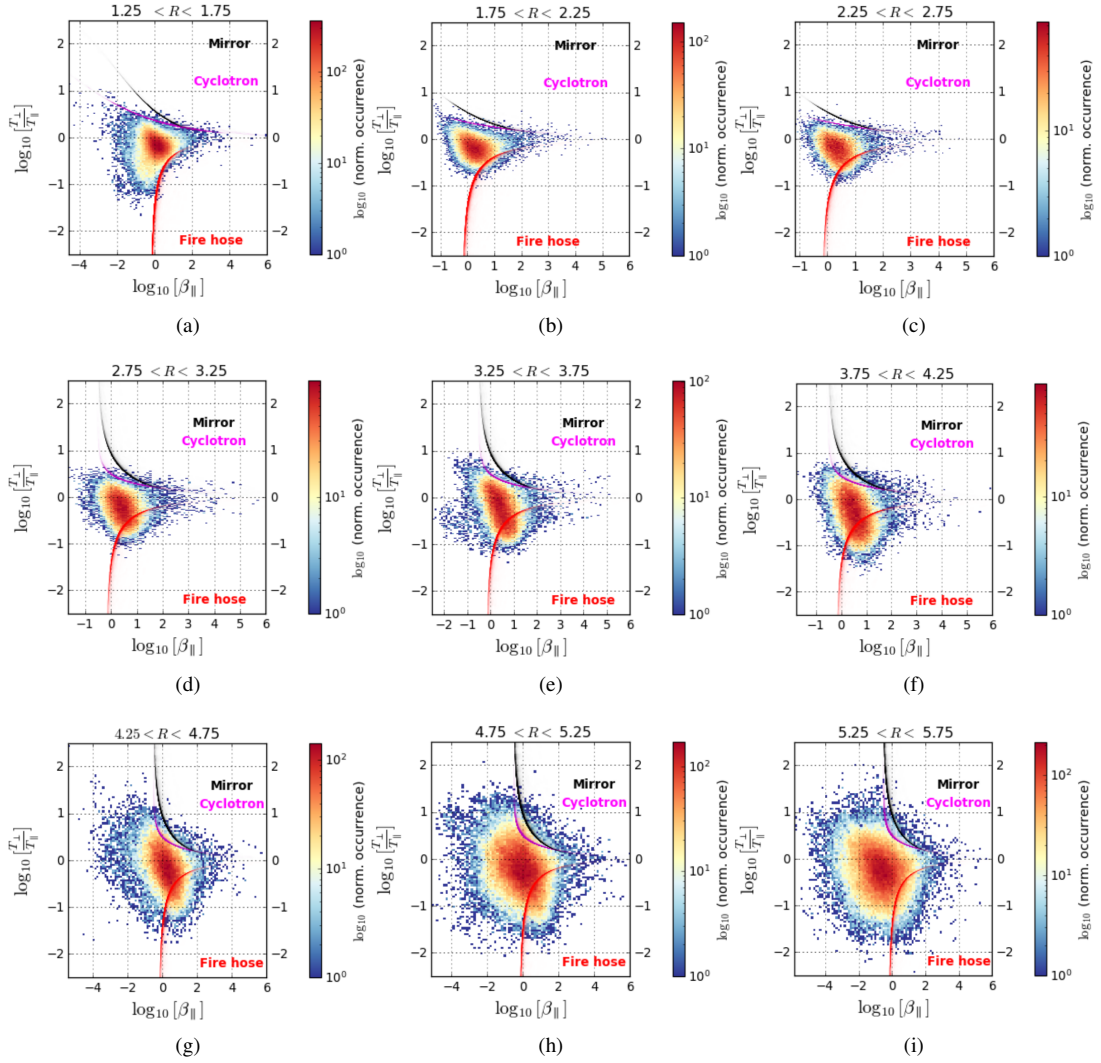


Figure 2: Logarithmic values of proton temperature anisotropy versus β_{\parallel} at different heliocentric distances. Curves indicate the firehose (red), mirror (black), and cyclotron (magenta) instabilities

This study highlights the significance of anisotropic cascades and temperature anisotropies driven by the background magnetic field and varying wave vectors in turbulent plasma. The Ulysses spacecraft data, covering heliocentric distances from 1.25 to 5.4 au, show how instabilities like the firehose and mirror modes affect the redistribution of energy within the solar wind, driven by temperature anisotropies relative to the magnetic field. The study finds that firehose instability plays a dominant role in the regulation of proton anisotropy between 3.25 au and 4.5 au, where the solar wind approaches a marginally stable state. Our results show that in this region the temperature anisotropy ratio lies within the range $0.6 < T_{\perp p}/T_{\parallel p} < 0.9$, which is typical of the mean stream component of the solar wind. The average anisotropy in this range is approximately $T_{\perp p}/T_{\parallel p}$ is 0.85, consistent with earlier studies [20, 21]. The presence of these instabilities facilitates an understanding of space weather and heliospheric conditions. This study provides crucial insights to understand energy transfer, wave-particle interactions, and space weather impacts, as its temperature and velocity anisotropies drive key instabilities and turbulence in space plasmas.

References

- [1] E. Marsch, “Kinetic Physics of the Solar Corona and Solar Wind,” *Living Reviews in Solar Physics*, vol. 3, no. 1, p. 1, Dec. 2006.
- [2] D. Stansby, D. Perrone, L. Matteini, T. S. Horbury, and C. S. Salem, “Alpha particle thermodynamics in the inner heliosphere fast solar wind,” *A&A*, vol. 623, p. L2, Mar. 2019.
- [3] P. Goldreich and S. Sridhar, “Toward a Theory of Interstellar Turbulence. II. Strong Alfvénic Turbulence,” *ApJ*, vol. 438, p. 763, Jan. 1995.
- [4] C. H. K. Chen, S. D. Bale, C. Salem, and F. S. Mozer, “Frame Dependence of the Electric Field Spectrum of Solar Wind Turbulence,” *ApJ*, vol. 737, no. 2, p. L41, Aug. 2011.
- [5] S. P. Gary and M. A. Lee, “The ion cyclotron anisotropy instability and the inverse correlation between proton anisotropy and proton beta,” *J. Geophys. Res.*, vol. 99, no. A6, pp. 11 297–11 302, Jun. 1994.
- [6] M. W. Kunz, A. A. Schekochihin, and J. M. Stone, “Firehose and Mirror Instabilities in a Collisionless Shearing Plasma,” *Phys. Rev. Lett.*, vol. 112, no. 20, p. 205003, May 2014.
- [7] K. B. Quest and V. D. Shapiro, “Evolution of the fire-hose instability: Linear theory and wave-wave coupling,” *J. Geophys. Res.*, vol. 101, no. A11, pp. 24 457–24 470, Nov. 1996.
- [8] P. Hellinger and H. Matsumoto, “New kinetic instability: Oblique Alfvén fire hose,” *J. Geophys. Res.*, vol. 105, no. A5, pp. 10 519–10 526, May 2000.
- [9] P. Hellinger, P. Trávníček, J. C. Kasper, and A. J. Lazarus, “Solar wind proton temperature anisotropy: Linear theory and WIND/SWE observations,” *Geophys. Res. Lett.*, vol. 33, no. 9, p. L09101, May 2006.
- [10] S. D. Bale, J. C. Kasper, G. G. Howes, E. Quataert, C. Salem, and D. Sundkvist, “Magnetic Fluctuation Power Near Proton Temperature Anisotropy Instability Thresholds in the Solar Wind,” *Phys. Rev. Lett.*, vol. 103, no. 21, p. 211101, Nov. 2009.
- [11] S. P. Gary, H. Li, S. O’Rourke, and D. Winske, “Proton resonant firehose instability: Temperature anisotropy and fluctuating field constraints,” *J. Geophys. Res.*, vol. 103, no. A7, pp. 14 567–14 574, Jul. 1998.
- [12] J. C. Kasper, A. J. Lazarus, and S. P. Gary, “Wind/SWE observations of firehose constraint on solar wind proton temperature anisotropy,” *Geophys. Res. Lett.*, vol. 29, no. 17, p. 1839, Sep. 2002.
- [13] O. A. Pokhotelov, R. Z. Sagdeev, M. A. Balikhin, and R. A. Treumann, “Mirror instability at finite ion-Larmor radius wavelengths,” *Journal of Geophysical Research (Space Physics)*, vol. 109, no. A9, p. A09213, Sep. 2004.
- [14] S. P. Gary, R. M. Skoug, J. T. Steinberg, and C. W. Smith, “Proton temperature anisotropy constraint in the solar wind: ACE observations,” *Geophys. Res. Lett.*, vol. 28, no. 14, pp. 2759–2762, Jul. 2001.
- [15] E. Marsch, “Waves and Turbulence in the Solar Corona,” in *The Sun and the Heliosphere as an Integrated System*, ser. Astrophysics and Space Science Library, G. Poletto and S. T. Suess, Eds., vol. 317, Nov. 2004, p. 283.
- [16] S. J. Bame, D. J. McComas, B. L. Barraclough, J. L. Phillips, K. J. Sofaly, J. C. Chavez, B. E. Goldstein, and R. K. Sakurai, “The ULYSSES solar wind plasma experiment,” *A&AS*, vol. 92, no. 2, pp. 237–265, Jan. 1992.
- [17] A. Balogh, T. J. Beek, R. J. Forsyth, P. C. Hedgecock, R. J. Marquedant, E. J. Smith, D. J. Southwood, and B. T. Tsurutani, “The magnetic field investigation on the ULYSSES mission - Instrumentation and preliminary scientific results,” *A&AS*, vol. 92, no. 2, pp. 221–236, Jan. 1992.
- [18] D. J. McComas, H. O. Funsten, J. T. Gosling, and W. R. Pryor, “Ulysses measurements of variations in the solar wind-interstellar hydrogen charge exchange rate,” *Geophys. Res. Lett.*, vol. 26, no. 17, pp. 2701–2704, Sep. 1999.
- [19] G. F. Chew, M. L. Goldberger, and F. E. Low, “The Boltzmann Equation and the One-Fluid Hydromagnetic Equations in the Absence of Particle Collisions,” *Proceedings of the Royal Society of London Series A*, vol. 236, no. 1204, p. 117, Jul. 1956.

- [20] R. von Steiger and T. H. Zurbuchen, “Temperature Anisotropies of Heavy Solar Wind Ions from Ulysses-SWICS,” in *Solar Wind Ten*, ser. American Institute of Physics Conference Series, M. Velli, R. Bruno, F. Malara, and B. Bucci, Eds., vol. 679. AIP, Sep. 2003, pp. 526–529.
- [21] E. T. Desta, R. D. Strauss, and N. E. Engelbrecht, “Modeling of the Polytropic Index and Temperature Anisotropy in the Solar Wind,” *ApJ*, vol. 966, no. 1, p. 142, May 2024.
- [22] L. Matteini, S. Landi, P. Hellinger, F. Pantellini, M. Maksimovic, M. Velli, B. E. Goldstein, and E. Marsch, “Evolution of the solar wind proton temperature anisotropy from 0.3 to 2.5 AU,” *Geophys. Res. Lett.*, vol. 34, no. 20, p. L20105, Oct. 2007.
- [23] L. Matteini, P. Hellinger, B. E. Goldstein, S. Landi, M. Velli, and M. Neugebauer, “Signatures of kinetic instabilities in the solar wind,” *Journal of Geophysical Research (Space Physics)*, vol. 118, no. 6, pp. 2771–2782, Jun. 2013.